

Accuracy Improvements in Microwave Noise Parameter Measurements

ANDREW C. DAVIDSON, BERNARD W. LEAKE, MEMBER, IEEE,
AND ERIC STRID, MEMBER, IEEE

Abstract—Factors contributing to microwave noise parameter measurement accuracy have been examined theoretically and experimentally. It is shown that for good accuracy the test source impedances need not be grouped around the impedance that produces minimum noise figure. System calibration and DUT *S*-parameter accuracy are important to the derived noise parameter accuracy, and the use of a vector network analyzer is advantageous. A new algorithm has been implemented which avoids errors caused by different noise source “on” and “off” impedances.

I. INTRODUCTION

ALTHOUGH NOISE parameter measurements are critical for low-noise microwave circuit design and device characterization, means of gathering accurate noise parameters have not been generally available. The result is that measured noise parameters are often doubted [1], FET noise modeling theories remain unverified [2], and progress in low-noise device development is generally hampered. In this paper we examine various factors which contribute to inaccuracies in noise parameter measurements, and illustrate effective solutions.

II. NOISE PARAMETER MEASUREMENT

The classic noise-parameter measurement system uses a manual or automated tuner on each end of the device under test (DUT). The tuners are intended to simulate the input and output matching networks of a low-noise amplifier stage so that the noise figure and gain can be measured directly.

If the input tuner is set for minimum indicated noise figure, the resulting tuning condition minimizes the combined loss of the tuner and the noise contributions of the DUT and the second stage. Since most tuners exhibit more loss with increasing reflection coefficient, the typical result is that the apparent optimum source reflection coefficient magnitude is too low [3]. The second-stage noise contribution is often significant; in some cases it is possible that source tuning for minimum overall noise figure will result in maximizing the DUT gain rather than minimizing its noise figure.

Manuscript received April 6, 1989; revised June 7, 1989.
The authors are with Cascade Microtech, Inc., 14255 S. W. Brigadoon Court, Beaverton, OR 97005.
IEEE Log Number 8930945.

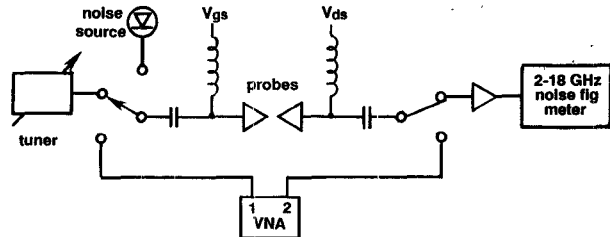


Fig. 1. Combined *S*-parameter and noise parameter measurement system.

Using Network Vector Information

The system shown in Fig. 1 (Cascade Microtech NPT18) has been used in the present work. To more accurately determine the optimal tuning conditions, the input tuner is switched between a set of predetermined impedance points instead of searching for the optimum [4]–[6]. Measurement speed is improved and device oscillation avoided by terminating the output of the DUT in a broad-band low-noise amplifier. Mismatch between the DUT output and the amplifier input is calculated from DUT *S* parameters and the input reflection coefficient of the receiver. To measure the DUT *S* parameters, source tuner impedances, and other mismatches and losses of the system, a vector network analyzer is switched into the DUT ports. Vector reflection information provides more accuracy than is available from scalar data.

To characterize the system, the vector network analyzer is first calibrated at the DUT connection planes. Then, for all test frequencies, source impedances presented to the DUT are measured for each tuner setting and for the hot noise source. The available gain of the two-port which connects the external calibrated hot noise source to the DUT is calculated to allow transfer of the excess noise ratio (ENR) calibration to the DUT input. The input impedance of the second-stage receiver is also measured. Noise parameters of the second stage are calculated from noise power measurements with a through-connect substituted for the DUT.

The calibrated noise source is the prime standard which determines the ultimate accuracy of F_{\min} and R_n . The

TABLE I
NOISE PARAMETERS USED IN SIMULATION

$$F_{\min} = 1.5 \text{ dB}$$

$$\Gamma_{\text{opt}} = .75 \angle 0^\circ$$

$$\beta = \frac{4R_n}{Z_0} \frac{1}{|1 + \Gamma_{\text{opt}}|^2} = 2.7$$

$$F = F_{\min} + \frac{4R_n}{Z_0} \cdot \frac{|\Gamma_{\text{opt}} - \Gamma_s|^2}{|1 + \Gamma_{\text{opt}}|^2 (1 - |\Gamma_s|^2)}$$

other noise parameters are obtained from relative measurements and so are not affected by noise source power calibration errors.

To characterize a DUT, its S parameters are measured. Then one measurement is made of noise power with the hot noise source connected, followed by a number of noise power measurements with other source impedances at ambient temperature. These measurements provide all the information necessary to calculate the overall system noise parameters and the DUT noise parameters and associated gain.

III. SOURCE IMPEDANCES: WHERE AND HOW MANY

Measurements for a minimum of four source impedances are necessary to solve for the four noise parameters F_{\min} , G_{opt} , B_{opt} , and R_n , but more are advantageous to allow averaging and help ensure a unique solution. To lend insight into the problem of noise parameter sensitivity to measurement errors, a computer simulation of noise figure measurements for a wide variety of source impedance configurations has been made. Topics of interest are how the source impedances should be distributed and how many are needed to optimize for accuracy and measurement speed.

The noise parameters of a typical FET (Table I) were used to calculate noise figure for each of a chosen set of source impedance points, and each noise factor was then assigned a random error of up to 1 percent. The resulting noise figures were then used to calculate the noise parameters using a least-squares routine [4], [5]. The differences between the calculated parameters and the original parameters are the errors which were RMS averaged over 400 runs.

The simulations presented here used source constellations forming a cross shape on the Smith chart. Fig. 2 shows two orientations of a nine-point set. Parameters which describe such a constellation are the maximum reflection coefficient of the outer source points (Γ_{\max}), the angular orientation (θ_{con}), and the number of source points. In all cases, one of the points was positioned at the center of the Smith chart, while the remainder were spaced equally along the lines forming the cross. The angular orientation of the source constellation was varied in the simulation because physical tuners will likely be distanced from the

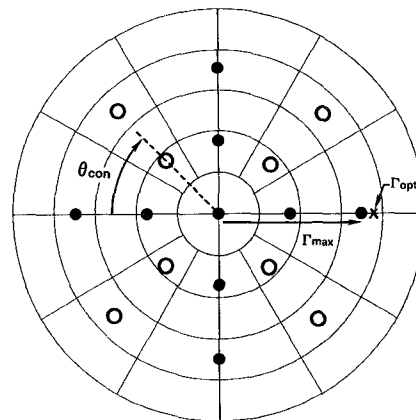


Fig. 2. Two source constellations used in the simulation.

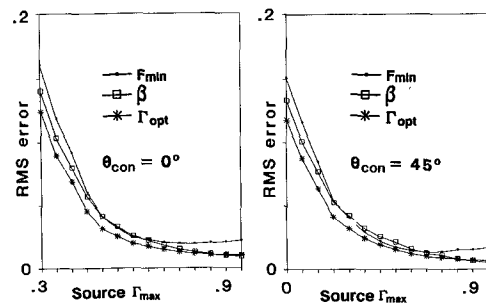


Fig. 3. Errors in predicted noise parameters versus maximum source reflection coefficient.

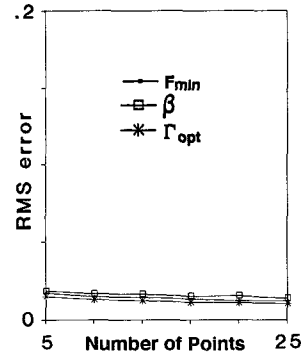


Fig. 4. Noise parameter errors versus number of source points.

DUT by lengths of transmission line, causing the orientation to change rapidly with frequency.

Fig. 3 shows the errors in predicted noise parameters as functions of Γ_{\max} for extreme orientations of the source points. It is interesting that, in this case, orientation of the source points has little effect on accuracy in spite of the fact that the nearest source can be quite far from gamma-opt. Larger source constellations generally produce better accuracy, but improvement is small beyond a magnitude somewhat less than gamma-opt. Fig. 4 shows that, for a given constellation, increasing the number of *intermediate* points does not help significantly, in contrast to increasing the averaging at a fixed point by a factor N , which would reduce the error there by a factor $1/\sqrt{N}$.

Another simulation was run in which all points in an initial constellation were made to converge on gamma-opt

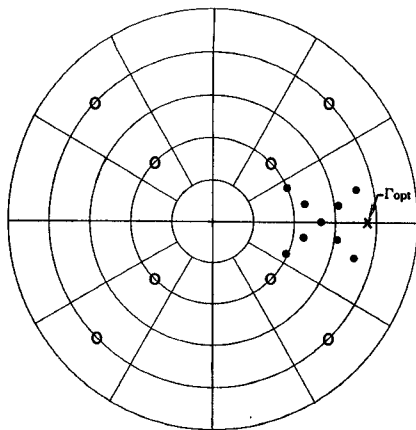


Fig. 5. Two configurations: The smaller corresponds to a scale factor of 0.7, the larger to a scale factor of 0.

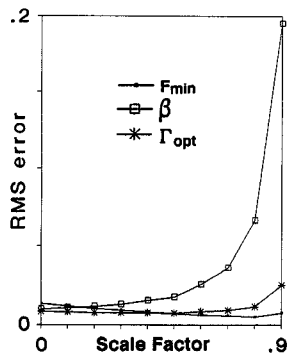


Fig. 6. Noise parameter errors versus proximity of source points to Γ_{opt} .

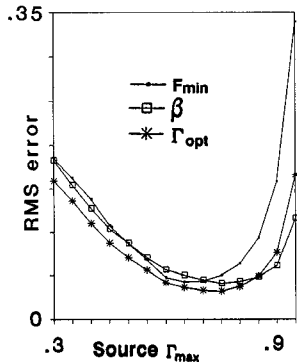


Fig. 7. Noise parameter errors for errors in source reflection coefficients.

by use of a scale factor, as shown in Fig. 5. Results plotted in Fig. 6 show that errors in β become large as the source constellation shrinks, while the other parameters change only slightly. This is expected, because β describes how rapidly the noise figure varies with Γ_s .

An example of the effect of source positional uncertainty is shown in Fig. 7, which is similar to Fig. 3 except that random source reflection coefficient errors were used instead of noise figure errors. The large errors for large Γ_{max} are expected because as a source impedance gets closer to the edge of the Smith chart, the gradient of the noise surface increases and small errors in source reflection

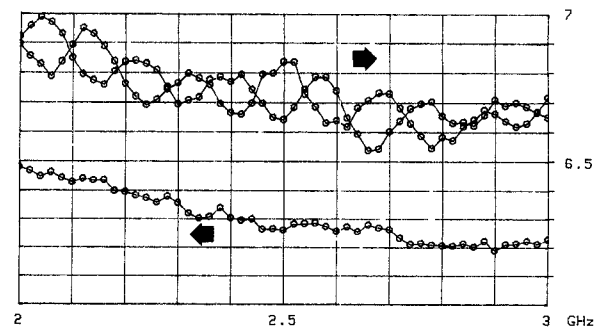


Fig. 8. Receiver F_{min} versus frequency, with and without the assumption that $\Gamma_{\text{HOT}} = \Gamma_{\text{COLD}}$.

coefficient cause large errors in noise figure. One possible way to reduce this effect would be to use an orthogonal fitting routine [6].

A. S-Parameter Accuracy

Network analyzer calibration and probe placement errors [7], [8], which are known to cause S-parameter inaccuracies, can seriously affect computed noise parameter accuracy. Modern low-noise devices are poorly matched to the normal reference impedance, which results in high- Q circuits.

B. Noise Source ON/OFF Impedance Change

Some procedures used in the derivation of noise parameters require the measurement of noise figures for a number of different source impedances. The noise figure is obtained from measurements of the noise powers (P_{hot} , P_{cold}) at the output of the receiver under test when its input is connected to a source which may be set to two substantially different known effective temperatures. The noise figure (F) is calculated from the equation

$$F = \frac{\text{ENR}}{Y - 1}$$

where ENR is the source excess noise ratio, and $Y = P_{\text{hot}}/P_{\text{cold}}$. Accuracy of the resultant noise figure relies on the total receiver gain and noise figure remaining constant between measurements of P_{hot} and P_{cold} , and this requires that the source impedance not change with effective temperature of the source [9], [10].

An improvement to this technique [11] points out that if the receiver input reflection coefficient is known, only one measurement of noise figure is necessary together with several "cold" noise power measurements. This method was used in the calibration of a noise characterization system (Fig. 1) using a 15 dB ENR source. In Fig. 8, the two upper traces show the effect of moving the noise source with a small coaxial extender. The ripples are caused by the difference in noise source "on" and "off" reflection coefficients, which was 0.05 magnitude.

A further improvement (see the Appendix) shows that when a number of cold noise power measurements are made for different source impedances, it is not necessary to measure cold noise power at the source impedance

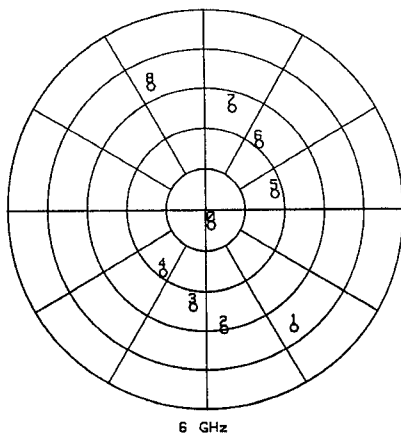
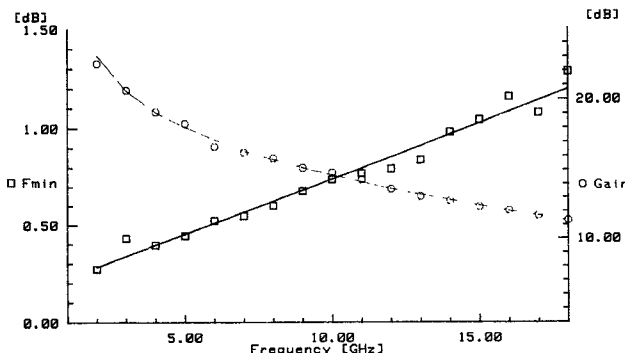
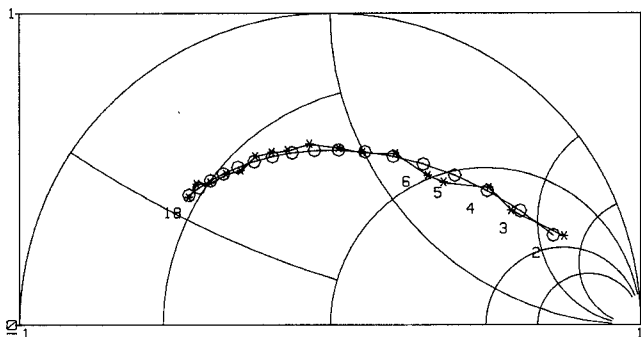


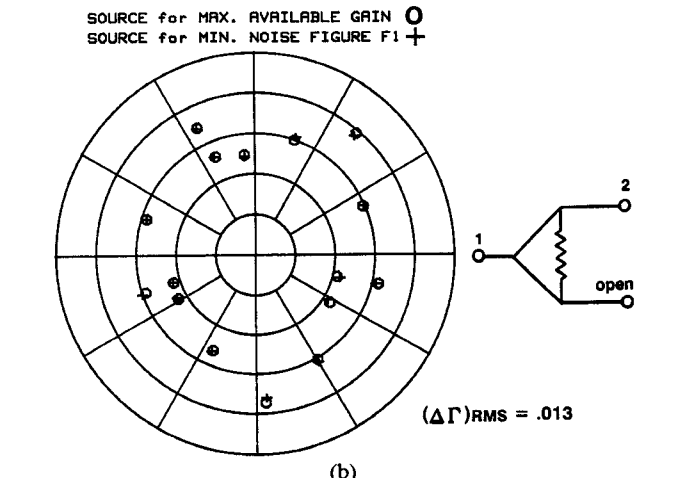
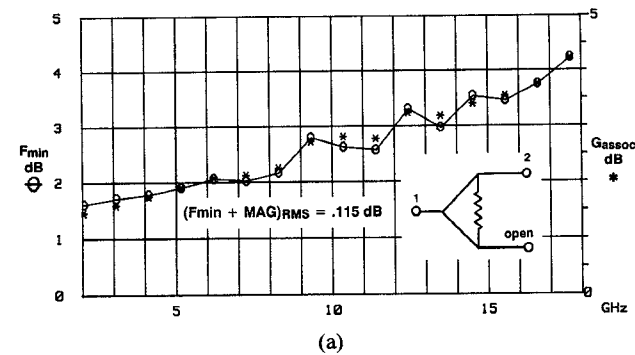
Fig. 9. Configuration of source points used in measurements at 6 GHz.

Fig. 10. F_{\min} and associated gain of a HEMT from measured data.Fig. 11. Γ_{opt} of a HEMT, 2-18 GHz: Measured *, smoothed O.

produced by the hot source. An implementation of this technique to a repeat calibration resulted in the lower trace in Fig. 8, which exhibits essentially no ripple.

IV. ACTIVE DEVICE MEASUREMENT

The ideas described above have been applied to the measurement of active devices. A typical $.25 \times 300 \mu\text{m}^2$ HEMT was measured over the frequency band 2 to 18 GHz, using nine source impedances as shown in Fig. 9 for 6 GHz. Figs. 10 and 11 show F_{\min} , associated gain, and Γ_{opt} using data which were obtained in less than seven seconds for each frequency. Groups of eight and seven points from the same measurements were fitted and found to give F_{\min} typically within 0.05 dB of the values obtained with all nine source points.

Fig. 12. A passive two-port verification. (a) F_{\min} (O); maximum available gain (*). (b) Gamma-opt: noise (+); available gain (O).

V. VERIFICATION

Measurement of a passive two-port can provide some assurance that the measurement system is working properly. The useful property of such a two-port is that $F = 1/G_{\text{av}}$ and the source for minimum noise figure and that for maximum available gain are the same. This test is not affected by noise source calibration errors, provided the same noise source is used to obtain the second stage and overall noise parameters, because $F_2/F_{12} = G_{\text{av}}$ in this case. The results of a passive verification are shown in Fig. 12.

VI. CONCLUSIONS

The combination of noise measurement instruments, together with a vector network analyzer, allows accurate determination of linear two-port noise parameters. System calibration, including S parameters and receiver noise parameters, removes uncertainties often associated with noise characterization measurements.

Computer simulations indicate that, in a system using a number of fixed source impedances, the principal concern in choosing a constellation is not the number of source points but rather their distribution on the Smith chart. If the points are well distributed, the noise figure surface will be described accurately even though measurements were not necessarily made close to the optimum. Given that measurement time is proportional to the number of points,

there is clear advantage to fewer, well placed source impedances which yield good results independent of the location of the optimum.

A procedure which avoids the need to measure noise figure (or P_{on} and P_{off} for the same source impedance) has been described, so differences between noise source hot and cold impedances are irrelevant.

The noise parameter system described, using on-wafer measurements of modern devices, results in smooth (within 0.1 dB) values of F_{min} with frequency and has high throughput.

APPENDIX

The ratio of the receiver gain (G_S) for a source reflection coefficient Γ_S to that (G_{REF}) with a perfectly matched source ($\Gamma_S = 0$) is given by

$$\frac{G_S}{G_{REF}} = \frac{1 - |\Gamma_S|^2}{|1 - \Gamma_S \Gamma_L|^2} = \frac{(P_H - P_C)_S}{(P_H - P_C)_{REF}} = g_s$$

where Γ_L is the receiver input reflection coefficient and P_H and P_C are the hot and cold noise powers.

The noise figure for any source impedance is given by

$$F_S = \frac{ENR}{Y-1} = \frac{ENR \cdot (P_C)_S}{(P_H - P_C)_S}. \quad (A1)$$

Therefore the ratio of the noise figures (F_1, F_2) for source reflection coefficients Γ_1 and Γ_2 is given by

$$\frac{F_1}{F_2} = \frac{(P_C/g)_1}{(P_C/g)_2} \quad (A2)$$

or

$$F_i = \frac{1}{k} \cdot \left(\frac{P_C}{g} \right)_i \quad (A3)$$

where k is a constant.

The noise figure (F_s) depends on the source admittance (Y_s) as given by

$$F_s = F_{min} + \frac{R_n}{G_s} |Y_s - Y_0|^2 \quad (A4)$$

where F_{min} , R_n , and $Y_0 = G_0 + jB_0$ are the noise parameters, which are independent of Y_s , the source admittance that produces the noise figure F_s . G_s is the real part of Y_s .

If F_s is scaled by a factor k , then

$$kF_s = kF_{min} + \frac{k \cdot R_n}{G_s} |Y_s - Y_0|^2. \quad (A5)$$

So F_{min} and R_n are also scaled by the same factor k while Y_0 , the source admittance that produces F_{min} , is unchanged.

Four, or more, measured values of $(P_C)_i$ with their corresponding values of g_i , calculated from $(\Gamma_S)_i$ and Γ_L , provide a set of values for kF_i that may be fitted to (A5) to obtain values for Y_0 , kF_{min} , and kR_n .

To find the scale factor, we proceed as follows. For the source reflection coefficient produced by the hot source,

from (A3),

$$k = \frac{(P_C/g)_0}{F_0}$$

which, from (A1), gives

$$k = \left[\left(\frac{P_H}{g} \right)_0 - \left(\frac{P_C}{g} \right)_0 \right] \cdot \frac{1}{ENR}.$$

Here g_0 is the relative gain; ENR is the hot source power calibration; $(P_C/g)_0 = kF_0$ is found from the four constants of (A5) and the source admittance Y_s produced by the hot source; and P_H is a new noise power measurement with the hot source.

Now that the scale factor k has been found, the known scaled noise parameters kF_{min} and kR_n can be scaled to F_{min} and R_n . The previously calculated Y_0 (which gives F_{min}) needs no scaling.

REFERENCES

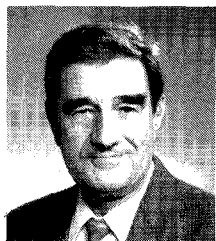
- [1] M. Pospieszalski *et al.*, "Comments on 'Design of microwave GaAs MESFET's for broadband, low-noise amplifier,'" *IEEE Trans. Microwave Theory Tech.*, vol. MTT-34, p. 194, Jan. 1986.
- [2] A. Cappy, "Noise modeling and measurement techniques," *IEEE Trans. Microwave Theory Tech.*, vol. 36, pp. 1-10, Jan. 1988.
- [3] E. Strid, "Measurement of losses in noise-matching networks," *IEEE Trans. Microwave Theory and Tech.*, vol. MTT-29, pp. 247-252, Mar. 1981.
- [4] R. Q. Lane, "The determination of device noise parameters," *Proc. IEEE*, vol. 57, pp. 1461-1462, Aug. 1969.
- [5] G. Caruso and M. Sannino, "Computer-aided determination of microwave two-port noise parameters," *IEEE Trans. Microwave Theory Tech.*, vol. MTT-26, pp. 639-642, Sept. 1978.
- [6] M. Mitama and H. Katoh, "An improved computational method for noise parameter measurement," *IEEE Trans. Microwave Theory Tech.*, vol. MTT-27, pp. 612-615, June 1979.
- [7] *Cascade Microtech Model 42 Operation Manual*, ch. 4. Cascade Microtech, Beaverton, OR.
- [8] K. Jones and E. Strid, "Where are my on-wafer reference planes?" in *IEEE ARFTG Dig.*, pp. 27-40, Dec. 1987.
- [9] E. Strid, "Noise measurements for low-noise GaAsFET amplifiers," *Microwave Syst. News*, part I, pp. 62-70, Nov. 1981; part II, Dec. 1981.
- [10] N. J. Kuhn, "Curing a subtle but significant cause of noise figure error," *Microwave J.*, vol. 27, pp. 85-98, June 1984.
- [11] A. Adamian and A. Uhlir, "A novel procedure for receiver noise characterization," *IEEE Trans. Instrum. Meas.*, vol. IM-22 pp. 181-182, June 1973.

+



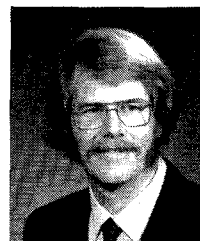
Andrew C. Davidson was born in Montreal, Canada, in 1963. He received the B.S. and M.Eng. degrees in applied and engineering physics from Cornell University, Ithaca, NY, in 1985 and 1987, respectively. During the year of 1986 he held an internship at Schlumberger Well Services, Houston, TX, where he characterized and modeled microwave slot antenna radiation in layered media.

He has been with Cascade Microtech, Beaverton, OR, since 1987, where he has been involved in the development of noise characterization systems.



Bernard W. Leake (M'57) was born in London, England, in 1928, and received the B.Sc degree in physics from London University in 1951.

Between 1957 and 1987 he worked on microwave systems and component design at Raytheon Equipment Division in Massachusetts. For some years his interests have included microwave computer-aided design and measurement. He is presently with Cascade Microtech, Beaverton, OR, where he is involved in computer-controlled characterization of low-noise devices.



Eric Strid (S'74-M'75) received the B.S.E.E. degree from the Massachusetts Institute of Technology, Cambridge, in 1974 and the M.S.E.E. degree from the University of California at Berkeley in 1975.

He first worked on microwave MIC's at Farnon Transmission Systems, San Carlos, CA. In 1979 he joined the GaAs research group at Tektronix. (This group evolved into TriQuint Semiconductor.) In 1983 he cofounded Cascade Microtech Inc., where he is now president and CEO. He has published various papers on power GaAs FET's, noise measurements, analog and digital GaAs IC's, and high-frequency wafer probing.